Atmos. Chem. Phys., 14, 4251–4262, 2014
www.atmos-chem-phys.net/14/4251/2014/
doi:10.5194/acp-14-4251-2014

Atmospheric Chemistry and Physics Open Access

Quantification of hydroxyacetone and glycolaldehyde using chemical ionization mass spectrometry

J. M. St. Clair[1], K. M. Spencer[2], M. R. Beaver[1,*], J. D. Crounse[1], F. Paulot[3,], and P. O. Wennberg[1,3]**

[1]Division of Geological and Planetary Sciences, California Institute of Technology, Pasadena, CA, USA
[2]Division of Chemistry and Chemical Engineering, California Institute of Technology, Pasadena, CA, USA
[3]Division of Engineering and Applied Science, California Institute of Technology, Pasadena, CA, USA
[*]now at: National Exposure Research Laboratory, Environmental Protection Agency, Research Triangle Park, NC, USA
[**]now at: Geophysical Fluid Dynamics Laboratory/National Oceanic and Atmospheric Administration, and Program in Atmospheric and Oceanic Sciences, Princeton University, Princeton, NJ, USA

Correspondence to: J. M. St. Clair (jstclair@caltech.edu)

Received: 26 July 2011 – Published in Atmos. Chem. Phys. Discuss.: 22 August 2011
Revised: 10 March 2014 – Accepted: 11 March 2014 – Published: 30 April 2014

Abstract. Chemical ionization mass spectrometry (CIMS) enables online, rapid, in situ detection and quantification of hydroxyacetone and glycolaldehyde. Two different CIMS approaches are demonstrated employing the strengths of single quadrupole mass spectrometry and triple quadrupole (tandem) mass spectrometry. Both methods are generally capable of the measurement of hydroxyacetone, an analyte with known but minimal isobaric interferences. Tandem mass spectrometry provides direct separation of the isobaric compounds glycolaldehyde and acetic acid using distinct, collision-induced dissociation daughter ions. The single quadrupole CIMS measurement of glycolaldehyde was demonstrated during the ARCTAS-CARB (Arctic Research of the Composition of the Troposphere from Aircraft and Satellites - California Air Resources Board) 2008 campaign, while triple quadrupole CIMS measurements of glycolaldehyde and hydroxyacetone were demonstrated during the BEARPEX (Biosphere Effects on Aerosols and Photochemistry Experiment) 2009 campaign. Enhancement ratios of glycolaldehyde in ambient biomass-burning plumes are reported for the ARCTAS-CARB campaign. BEARPEX observations are compared to simple photochemical box model predictions of biogenic volatile organic compound oxidation at the site.

1 Introduction

Carbonyl compounds make a large contribution to the production of free radicals and photooxidants in the atmosphere. Hydroxyacetone ($H_3CC(O)CH_2OH$) and glycolaldehyde ($HC(O)CH_2OH$) have both biogenic and biomass-burning sources. Both species are important oxidation products of isoprene (2-methyl-1,3-butadiene), and glycolaldehyde is also produced during the oxidation of 2-methyl-3-buten-2-ol (MBO). Isoprene is produced by deciduous plants and is the single largest source of nonmethane hydrocarbons to the atmosphere (Guenther et al., 1995) while MBO is emitted in large quantities from several species of pine (Goldan et al., 1993; Harley et al., 1998). Photooxidation of isoprene in the presence of NO produces methyl vinyl ketone (MVK) and methacrolein (MACR) (Tuazon and Atkinson, 1990a; Paulson et al., 1992). MVK and MACR are further oxidized to produce second-generation isoprene photooxidation products glycolaldehyde, hydroxyacetone, methylglyoxal ($H_3CC(O)CH(O)$), and formaldehyde (CH_2O) (Tuazon and Atkinson, 1989, 1990b). Recent studies suggest additional prompt sources of hydroxyacetone and glycolaldehyde during the isomerization of alkoxyradicals formed from isoprene photooxidation (Dibble, 2004a, b; Paulot et al., 2009a; Karl et al., 2009; Galloway et al., 2011; Peeters and Nguyen, 2012). Oxidation products of biogenic volatile organic compounds play a significant role in tropospheric ozone production (Chameides et al., 1988; Atkinson and Arey, 2003) and

formation of secondary organic aerosol (Kroll et al., 2006). Hydroxyacetone and glycolaldehyde are also emitted during biomass burning, and measurements of both have been reported for laboratory and field fires of various fuels (e.g., Akagi et al., 2011, 2012; Yokelson et al., 2013; Johnson et al., 2013).

Hydroxyacetone and glycolaldehyde are precursors of other atmospherically relevant species. Major products of hydroxyacetone and glycolaldehyde photooxidation are methylglyoxal and glyoxal (OCHCHO), respectively (Grosjean et al., 1993; Niki et al., 1987). Additionally, Butkovskaya et al. (2006a, b) found oxidation of hydroxyacetone and glycolaldehyde by OH yields formic acid while OH oxidation of hydroxyacetone also produces acetic acid.

Previous atmospheric measurements of hydroxyacetone and glycolaldehyde have been made using a range of analytical techniques. The most common of these involve ambient sample collection, derivatization with a chemical agent, separation of compounds, and detection by HPLC (high-performance liquid chromatography), GC–MS (gas chromatography–mass spectrometry), or GC-FID (gas chromatography–flame ionization detection) (Lee et al., 1993, 1995; Zhou et al., 2009; Moortgat et al., 2002; Spaulding et al., 2003; Matsunaga et al., 2003). Two shortcomings of these techniques are the intensive sample processing required and the time lag between sample collection and concentration measurement. Typical measurement periods are 5 min–2 h. In contrast, both single quadrupole and triple quadrupole (tandem) chemical ionization mass spectrometry (CIMS) enable online, rapid, in situ measurements with no sample processing. In these techniques, the ambient sample enters the instrument directly and reaches the detector rapidly (<1 s), enabling immediate detection of these compounds and providing a potentially high temporal resolution data set. Both the Caltech single quadrupole and tandem CIMS instruments can quantitatively measure hydroxyacetone, an analyte with a known but minor isobaric interference (propanoic acid) in the atmosphere. The Caltech tandem CIMS instrument enables direct separation of mass analogues glycolaldehyde and acetic acid. A similar method, proton-transfer-reaction mass spectrometry (PTRMS), has been used by Karl et al. (2009) to measure hydroxyacetone concentrations in the Amazon Basin. Infrared absorption has also been used to measure atmospheric glycolaldehyde and hydroxyacetone, particularly for biomass-burning plumes (Johnson et al., 2013). FTIR (Fourier Transform Infrared) spectroscopy provides a direct measurement with a faster measurement cycle than the derivatization techniques, though it cannot match the measurement cycle and sensitivity of the CIMS technique.

We present two sets of in situ measurements: airborne, boundary layer measurements of glycolaldehyde over portions of California; and tower-based measurements of glycolaldehyde and hydroxyacetone at a site approximately 80 km northeast of Sacramento, California. The first set of measurements was made in June of 2008 from the NASA DC-8 aircraft platform using the Caltech single quadrupole CIMS instrument during the California portion of the NASA-CARB (California Air Resources Board) Arctic Research of the Composition of the Troposphere from Aircraft and Satellites (ARCTAS-CARB) field experiment. The four ARCTAS-CARB flights included in this study (18, 20, 22, and 26 June) occurred during daytime hours. Enhancement ratios of glycolaldehyde in biomass-burning plumes are presented and compared to literature values for laboratory and field fire data. The second set of measurements was made during the Biosphere Effects on Aerosols and Photochemistry Experiment (BEARPEX) 2009 field experiment from 28 June to 20 July using the Caltech tandem CIMS instrument. The site is a ponderosa pine plantation (38°53′42.9″ N, 120°37′57.9″ W, elevation 1315 m), located near the University of California's Blodgett Forest Research Station, on the western slope of the Sierra Nevada. The site is approximately 5 h downwind of Sacramento and has been described in detail previously by Goldstein et al. (2000) and Dreyfus et al. (2002). The measurements presented here were conducted from the top platform of the north tower; the instrument inlet was located 17.8 m above the ground. Concentrations of hydroxyacetone and glycolaldehyde are compared to results from a simple photochemical box model used to estimate the contribution of biogenic sources to the budget of glycolaldehyde and hydroxyacetone at the site.

2 Instrumentation

2.1 Instrument description

Negative ion chemistry of CF_3O^- has been shown to provide sensitive detection of many atmospheric trace gases (Huey et al., 1996; Amelynck et al., 2000a, b; Crounse et al., 2006; Spencer et al., 2009; Paulot et al., 2009a, b; St. Clair et al., 2010) and was exploited in this work to detect hydroxyacetone, glycolaldehyde, acetic acid, and hydrogen cyanide (HCN). The measurement of HCN by the Caltech single quadrupole CIMS has been described previously (Crounse et al., 2006, 2009). The use of CF_3O^- to detect hydroxyacetone and glycolaldehyde was introduced briefly by Paulot et al. (2009a) and Chan et al. (2009) and is described in detail here. Hydroxyacetone and glycolaldehyde react with CF_3O^- via clustering between the reagent ion and the analyte through Reactions (R1) and (R2), respectively; mass-to-charge ratio is denoted by m/z. Acetic acid reacts with CF_3O^- via fluoride ion transfer through Reaction (R3) and clustering through Reaction R4, providing two distinct ion signals. Reactions (R1–R4) are complicated by competing reactions with CF_3O^- water cluster ($CF_3O^- \cdot H_2O$).

$$CF_3O^- + H_3CC(O)CH_2OH \rightarrow \quad \text{(R1)}$$

$$CF_3O^- \cdot H_3CC(O)CH_2OH \ (m/z\ 159)$$

$$CF_3O^- + HC(O)CH_2OH \rightarrow \quad \text{(R2)}$$

$$CF_3O^- \cdot HC(O)CH_2OH \ \ (m/z\ 145)$$

$$CF_3O^- + H_3CC(O)OH \rightarrow \quad \text{(R3)}$$

$$H_3CC(O)O^- \cdot HF \ \ (m/z\ 79) + CF_2O$$

$$CF_3O^- + H_3CC(O)OH \rightarrow \quad \text{(R4)}$$

$$CF_3O^- \cdot H_3CC(O)OH \ \ (m/z\ 145)$$

The two Caltech CIMS instruments are described in brief below. A more detailed description of the single quadrupole and tandem CIMS instruments are available in Crounse et al. (2006) and St. Clair et al. (2010), respectively. Sample air enters the flow tube of the Caltech single quadrupole CIMS instrument and is diluted approximately 1 : 4 with ultra-high purity N_2. Flow tube pressure is maintained at 35 hPa. The reagent ion, CF_3O^-, is generated by flowing a mixture of ultra-high purity N_2 and the reagent ion precursor, CF_3OOCF_3, through a Po-210 source. The CF_3O^- is introduced perpendicular to the sample flow. Ions are sampled from the ion–molecule reaction volume into high vacuum where they are guided to a quadrupole mass filter and detected with a channel electron multiplier. Each mass-to-charge ratio is observed for ∼0.5 s. HCN, glycolaldehyde, and acetic acid masses were monitored once every ∼15 s during ARCTAS-CARB. As in the single quadrupole CIMS instrument, the flow tube of the tandem CIMS instrument is maintained at 35 hPa total pressure. During the BEARPEX campaign, ambient air was diluted 1 : 7 with liquid nitrogen boil-off. The tandem CIMS instrument contains three quadrupoles. The first quadrupole filters ions for a specific mass-to-charge ratio. These ions then enter the second quadrupole, which serves as a collision-induced dissociation (CID) chamber. The pressure in this quadrupole is maintained at 2.7×10^{-3} hPa N_2. Ions that reach this chamber collide with N_2 molecules and fragment into daughter ions. The third quadrupole selects for a specific daughter ion. Each mass-to-charge ratio is observed for ∼1 s. Hydroxyacetone, glycolaldehyde, and acetic acid masses were monitored once every ∼25 s.

2.2 Calibration and sensitivity

Due to differences in the reactivity of the analyte with CF_3O^- and $CF_3O^- \cdot H_2O$, the sensitivity of the Caltech CIMS instrumentation to the ion products of Reactions (R1–R4) varies with the mixing ratio of water vapor present in the flow tube. H_2O can also displace (ligand switching) or hydrolyze the analyte anion. The dependence of instrument sensitivity on water vapor mixing ratio was quantified during laboratory calibrations. The ion signal was determined as a function of humidity to obtain a water-dependent sensitivity curve. In all calibrations, mass flow controllers were used to control the flow tube humidity by adjusting the ratio of moist N_2 to dry N_2. Humidity was quantified by FTIR spectroscopy using HITRAN (high-resolution transmission) line lists (Rothman et al., 2005) and the nonlinear fitting software NLM4 developed by Griffith (1996). All analyte sensitivities were corrected for background signals.

For calibrations, hydroxyacetone and glycolaldehyde standards were prepared by serial dilution. Gas-phase hydroxyacetone was produced by flowing dry N_2 over commercially available, 95 % pure hydroxyacetone (Alfa Aesar) into a 150 L Teflon bag. Additional dry N_2 was added to the bag such that the final concentration of hydroxyacetone was 150 ppmv (parts per million by volume). Initially, the hydroxyacetone concentration was determined by both FTIR absorption (Orlando et al., 1999) and quantification of the mass loss of the liquid. These methods agreed within 25 %; the concentration determined by mass loss was higher than that determined by FTIR absorption. In calibration experiments, hydroxyacetone concentration was determined by mass loss alone as the FTIR instrument was dedicated to the determination of water vapor concentration. From the 150 L bag, 150 mL were quantitatively transferred to a 400 L Teflon bag. A known quantity of dry N_2 was added such that the concentration of hydroxyacetone was 50 ppbv (parts per billion by volume) in the 400 L bag.

Similarly, gas-phase glycolaldehyde was transferred to a 100 L Teflon bag by flowing dry N_2 over glycolaldehyde dimer (Fluka Analytical) while gently heating the compound. Additional dry N_2 was added to the bag such that the concentration of glycolaldehyde was 100 ppmv. The glycolaldehyde concentration was determined by both FTIR absorption (Tuazon and Atkinson, 1989) and quantification of the mass loss of the solid. These methods agreed within 45 %; the concentration determined by mass loss was higher than that determined by FTIR absorption. During calibration experiments, as mentioned above for hydroxyacetone, the FTIR was used to determine water vapor concentration and so the glycolaldehyde concentration was determined by mass loss alone. From the 100 L bag, 300 mL were quantitatively transferred to a 400 L Teflon bag. Dry N_2 was added to give a final glycolaldehyde concentration of 75 ppbv.

For acetic acid calibrations, a ^{13}C isotopically labeled standard was used. The acetic acid evolved from a permeation tube that was held at a constant temperature (Washenfelder et al., 2003), and the permeation rate was determined by mass loss.

Calibrations of hydroxyacetone, glycolaldehyde, and acetic acid were conducted separately, but the method was similar for all calibrations. A known quantity of analyte from the standards discussed above was combined with water vapor and N_2 dilution gas in the instrument flow tube. The CIMS instrument signal was monitored as a function of water vapor in the flow tube to develop the instrument sensitivity curve. The sensitivities of the single quadrupole CIMS instrument to the cluster channel of hydroxyacetone (*m/z* 159), the cluster channel of glycolaldehyde (*m/z* 145),

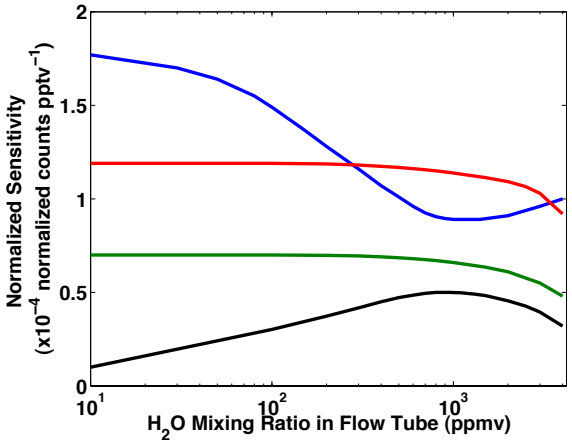

Fig. 1. Single quadrupole CIMS instrument sensitivity curves for hydroxyacetone (red), glycolaldehyde (green), acetic acid fluoride transfer product (blue), and acetic acid cluster product (black) as a function of H_2O mixing ratio in the instrument flow tube. The sensitivity curves are used to calculate the final concentrations of the analytes.

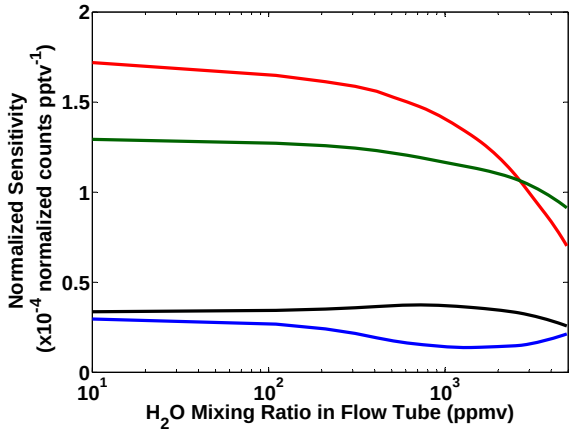

Fig. 2. Tandem CIMS instrument sensitivity curves for hydroxyacetone daughter ion $m/z = 159 \rightarrow m/z = 85$ (red), glycolaldehyde daughter ion $m/z = 145 \rightarrow m/z = 85$ (green), acetic acid fluoride transfer daughter ion $m/z = 79 \rightarrow m/z = 59$ (blue), and acetic acid cluster daughter ion $m/z = 145 \rightarrow m/z = 79$ (black) as a function of the H_2O mixing ratio in the instrument flow tube. The sensitivity curves are used to calculate the final concentrations of the analytes. Typical H_2O mixing ratio values in the instrument flow tube were approximately 1500 ppmv during the BEARPEX campaign.

the fluoride transfer channel of acetic acid (*m/z* 79), and the cluster channel of acetic acid (*m/z* 145) are shown in Fig. 1. The sensitivity of the tandem CIMS instrument to the hydroxyacetone daughter ion ($m/z = 159 \rightarrow m/z = 85$), glycolaldehyde daughter ion ($m/z = 145 \rightarrow m/z = 85$), acetic acid fluoride transfer daughter ion ($m/z = 79 \rightarrow m/z = 59$), and acetic acid cluster daughter ion ($m/z = 149 \rightarrow m/z = 79$) are shown in Fig. 2. Daughter ions produced in the CID chamber of the Caltech tandem CIMS instrument are discussed below in Sect. 3.2. Sensitivity is expressed in ion counts, normalized by the ion counts of the sum of ^{13}C and ^{17}O isotopes of the reagent ion and its one-water cluster, per pptv (parts per trillion by volume) of analyte. Daughter ions $m/z = 86 \rightarrow m/z = 86$, $m/z = 104 \rightarrow m/z = 86$, and $m/z = 104 \rightarrow m/z = 104$ of the reagent ions are used in normalization of the tandem CIMS instrument ion counts.

Post-field-campaign laboratory calibrations for hydroxyacetone, glycolaldehyde, and acetic acid were conducted for both the single quadrupole CIMS instrument and the tandem CIMS instrument. During the ARCTAS-CARB flights and the BEARPEX experiment, isotopically labeled acetic acid from the permeation tube was periodically added to the flow tube of the CIMS instruments to quantify the instrument sensitivity. The sensitivity of the single quadrupole CIMS instrument to acetic acid during the ARCTAS-CARB campaign was consistent with that of laboratory calibrations. The consistent sensitivity of the tandem CIMS instrument was similarly confirmed during the BEARPEX campaign and laboratory calibrations.

In the absence of hydroxyacetone, glycolaldehyde, and acetic acid, ion signals at their respective *m/z* are nonzero. Background signals were measured during field experiments by periodically passing ambient air through a filter consisting of a few alumina pellets coated with palladium followed by nylon wool coated with sodium bicarbonate, quantitatively removing hydroxyacetone, glycolaldehyde, and acetic acid. This technique is described in Crounse et al. (2006). Background signals were monitored approximately every 20 min during the ARCTAS-CARB flights and approximately every 45 min during the BEARPEX campaign.

3 Determination of analyte concentration

3.1 Single quadrupole CIMS Instrument

The single quadrupole CIMS instrument was used to conduct ambient measurements in and around California during the ARCTAS-CARB campaign. Determination of the ambient mixing ratios of glycolaldehyde, acetic acid, and HCN is discussed below. Ambient mixing ratios of these trace gases are calculated from the analyte ion signal after normalization by the amount of reagent ion signal, subtraction of background signals, and application of the appropriate sensitivity factor.

3.1.1 Hydroxyacetone

Hydroxyacetone clusters with the reagent ion CF_3O^- and is detected at *m/z* 159. There is a known atmospheric interference at that *m/z*: propanoic acid. Analogous to using *m/z* 79 to remove the acetic acid contribution to *m/z* 145 (Sect. 3.1.2), it is possible to use *m/z* 93 to remove the propanoic acid

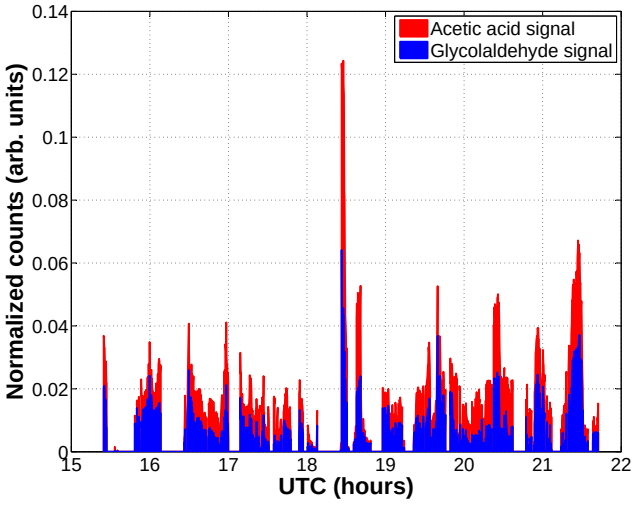

Fig. 3. A time series of the contribution of acetic acid and glycolaldehyde to the *m/z* 145 signal detected by the Caltech single quadrupole CIMS instrument during the 18 June 2008 flight. The *m/z* 145 signal due to acetic acid is estimated from the *m/z* 79 acetic acid signal. The signal due to glycolaldehyde is determined by subtracting the signal due to acetic acid from the total *m/z* 145 signal.

contribution to *m/z* 159. Because propanoic acid has not been observed in large quantities relative to hydroxyacetone outside of biomass-burning plumes, the *m/z* 159 data can generally be used for hydroxyacetone without correction.

3.1.2 Glycolaldehyde

The quantification of glycolaldehyde is complicated by a significant interference due to acetic acid, an exact mass analogue of glycolaldehyde. Both species undergo CF_3O^- clustering chemistry and are detected at *m/z* 145. Thus, the *m/z* 145 signal due to acetic acid in the form $CF_3O^- \cdot H_3CC(O)OH$ must be accounted for when determining the ambient glycolaldehyde concentration. This is accomplished by estimating the *m/z* 145 acetic acid signal from the acetic acid signal detected at *m/z* 79.

As discussed above, acetic acid also reacts with CF_3O^- via fluoride ion transfer and is detected as $H_3CC(O)O^- \cdot HF$ at *m/z* 79 (R3). There are no known interferences at this mass-to-charge ratio. The ratio of fluoride transfer ions (*m/z* 79) to clustering ions (*m/z* 145) for acetic acid is dependent on the amount of water in the instrument flow tube (Fig. 1). The ratio is determined experimentally via the laboratory and field calibrations discussed above. The *m/z* 145 signal due to acetic acid is estimated by multiplying the *m/z* 79 acetic acid signal by the water-dependent ratio of the acetic acid *m/z* 145 signal to the acetic acid *m/z* 79 signal. The average acetic acid contribution to the total *m/z* 145 signal ranged from 40 to 60 % over the four ARCTAS-CARB flights. The contributions of acetic acid and glycolaldehyde to the *m/z* 145 signal are shown for the 18 June 2008 flight in Fig. 3.

The *m/z* 145 signal due to glycolaldehyde is calculated by subtracting the *m/z* 145 signal due to acetic acid from the total *m/z* 145 signal detected by the single quadrupole CIMS instrument. The corrected glycolaldehyde signal is converted to concentration by application of the laboratory-determined instrument sensitivity factor for glycolaldehyde (Fig. 1, green curve). The uncertainty in the single quadrupole glycolaldehyde measurements is approximately $\pm$(60 % + 50 pptv). The uncertainty reflects the sum of the data precision determined by the counting statistics of the ions, the variability of the background signal, and the uncertainty in the sensitivity factors for glycolaldehyde and acetic acid shown in Fig. 1.

3.2 Tandem CIMS instrument

The tandem CIMS instrument was used to conduct ambient measurements at a tower site about 5 h downwind of Sacramento during the BEARPEX 2009 campaign. Determination of the ambient mixing ratios for hydroxyacetone, glycolaldehyde, and acetic acid is discussed below. Similar to measurements made using the single quadrupole instrument, ambient concentrations of these trace gases are calculated from the ion signals after normalization by the amount of reagent ion signal, subtraction of background signals, and application of the appropriate sensitivity factor. An advantage of tandem CIMS lies in the ability to differentiate between isobaric species provided their fragmentation patterns are sufficiently unique.

3.2.1 Hydroxyacetone

The MS/MS ion signal $m/z = 159 \rightarrow m/z = 85$ was used to measure hydroxyacetone with the tandem CIMS instrument. The uncertainty in the tandem hydroxyacetone measurements is approximately $\pm$(40 % + 50 pptv). The uncertainty reflects the sum of the precision of the data determined by the counting statistics of the ions, the variability of the background signal, and the uncertainty in the sensitivity factor shown in Fig. 2.

3.2.2 Glycolaldehyde

The advantages of tandem mass spectrometry are demonstrated in the separate quantification of the isobaric compounds glycolaldehyde and acetic acid. The sequence of quadrupole mass filter, CID chamber, and second quadrupole mass filter enables the decomposition of isobaric ions into daughter ion fragments. As discussed above, while operating in tandem MS mode, ions of a selected mass-to-charge ratio pass through the first quadrupole mass filter and into the CID chamber, where they collide with N_2 molecules and fragment into daughter ions. The second quadrupole mass filter selects daughter ions of a certain mass-to-charge ratio.

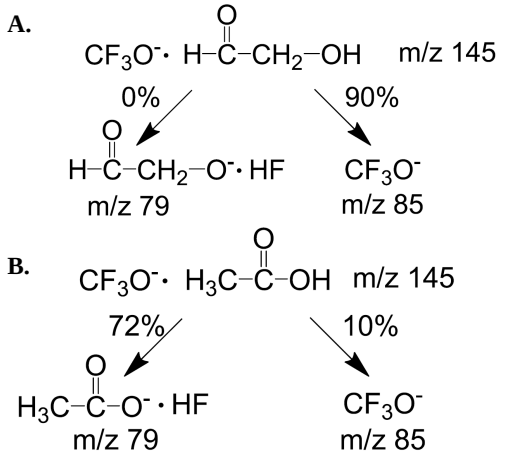

Fig. 4. Collision-induced dissociation fragmentation pattern of glycolaldehyde **(A)** and acetic acid **(B)** including the percentage of *m/z* 145 parent ions that fragment to each of the daughter ions. The orthogonality of daughter ions enables confident differentiation of glycolaldehyde and acetic acid.

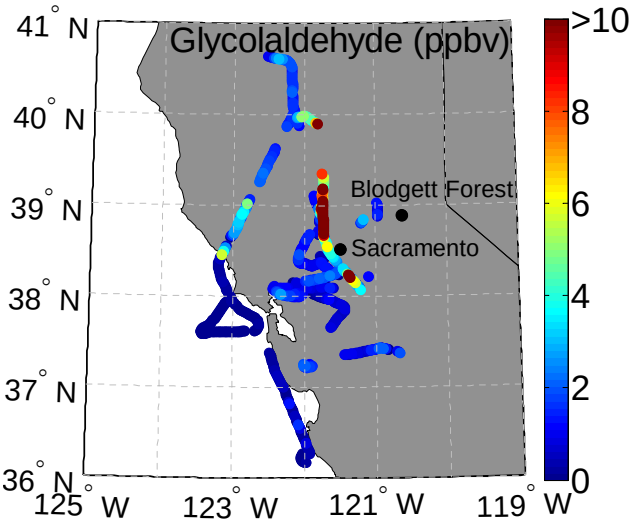

Fig. 5. ARCTAS-CARB flight tracks colored by glycolaldehyde. Data presented are those when pressure altitude is less than 1.5 km. Observed concentrations of glycolaldehyde are lowest along the coast and highest further inland, closer to biomass-burning and biogenic sources.

Glycolaldehyde and acetic acid CF_3O^- cluster ions fragment differently due to differences in the stabilities of their clusters and the resultant daughter fragments. Significant daughter ion signals were observed at *m/z* 79, *m/z* 85, and *m/z* 145 and are denoted $m/z = 145 \rightarrow m/z = 79$, $m/z = 145 \rightarrow m/z = 85$, and $m/z = 145 \rightarrow m/z = 145$, respectively. Figure 4 shows the parent ions – glycolaldehyde and acetic acid – and their significant daughter ion fragments for the collision energies used here. The daughter ion signals are reported relative to the sum of the three significant daughter ion signals for each compound. As shown in Fig. 4a, 90 % of glycolaldehyde *m/z* 145 parent ions fragment to *m/z* 85 daughter ions, and 0 % fragment to *m/z* 79 daughter ions. The predominate daughter ion of acetic acid *m/z* 145 parent ions is *m/z* 79 (72 %) (Fig. 4b). Ten percent of acetic acid *m/z* 145 parent ions fragment to *m/z* 85. Ten percent of glycolaldehyde and 18 % of acetic acid *m/z* 145 parent ions do not fragment and are detected at $m/z = 145 \rightarrow m/z = 145$. Acetic acid also fragments to $m/z = 145 \rightarrow m/z = 59$, but the ion signal is a factor of ten less than that observed at $m/z = 145 \rightarrow m/z = 79$.

Based on the fragmentation patterns, ambient signals due to glycolaldehyde and acetic acid are separated. The $m/z = 145 \rightarrow m/z = 85$ signal is mainly due to glycolaldehyde, and the small contribution due to acetic acid is accounted for during data analysis. The signal at $m/z = 145 \rightarrow m/z = 85$ due to acetic acid is calculated by multiplying the acetic acid signal at $m/z = 145 \rightarrow m/z = 79$ by the laboratory-derived ratio of acetic acid signal at $m/z = 145 \rightarrow m/z = 85$ to acetic acid signal at $m/z = 145 \rightarrow m/z = 79$. The $m/z = 145 \rightarrow m/z = 85$ signal due to glycolaldehyde is calculated by subtracting the acetic acid $m/z = 145 \rightarrow m/z = 85$ signal from the total $m/z = 145 \rightarrow m/z = 85$ signal.

Glycolaldehyde concentrations are calculated using the corrected glycolaldehyde $m/z = 145 \rightarrow m/z = 85$ ion signal and the corresponding tandem CIMS instrument sensitivity curve. Acetic acid concentrations are calculated using both the $m/z = 79 \rightarrow m/z = 59$ and $m/z = 145 \rightarrow m/z = 79$ ion signals and their respective sensitivity curves. The uncertainty in the tandem CIMS glycolaldehyde measurements is approximately ±(50 % + 50 pptv). The uncertainty in the tandem CIMS acetic acid measurements is approximately ±(40 % + 50 pptv). The uncertainties reflect the sum of the precision of the data determined by the counting statistics of the ions, the variability of the background signal, and the uncertainty in the sensitivity factors shown in Fig. 2.

3.3 Comparison of the two CIMS techniques

The Caltech single quadrupole CIMS instrument has higher ion transmission, and consequently higher sensitivity, than the tandem CIMS instrument. Measurement of an analyte by the single quadrupole instrument is therefore preferable to measurement by the tandem CIMS instrument, when there are no interferences at the observed *m/z*. For analytes such as glycolaldehyde, the benefit of the higher precision for the single quadrupole CIMS is offset by the uncertainty introduced by subtracting a portion of the signal due to interfering compounds. As the signal from the interfering compound constitutes a larger fraction of the total observed signal, the uncertainty in the final glycolaldehyde mixing ratio increases. Because acetic acid is much more prevalent in the atmosphere than propanoic acid, relative to glycolaldehyde and hydroxyacetone, respectively, the tandem CIMS technique benefits

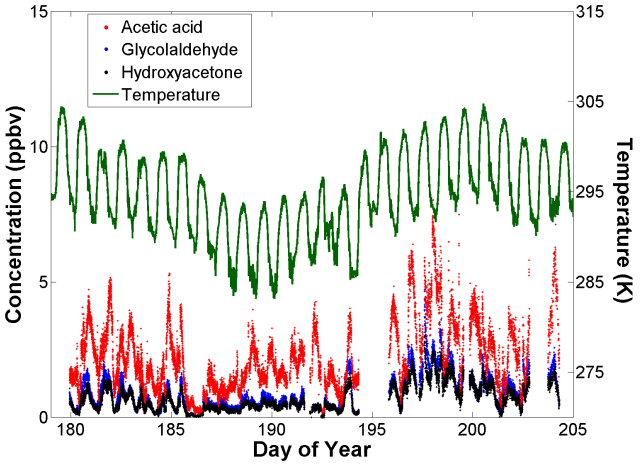

Fig. 6. Concentrations of acetic acid ($m/z = 145 \rightarrow m/z = 79$, red), glycolaldehyde ($m/z = 145 \rightarrow m/z = 85$, blue), and hydroxyacetone ($m/z = 159 \rightarrow m/z = 85$, black) measured using the Caltech tandem CIMS instrument during the BEARPEX 2009 campaign.

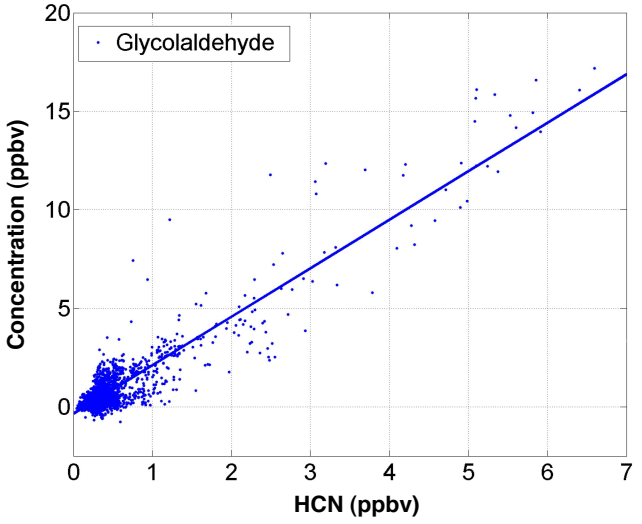

Fig. 7. Correlation between glycolaldehyde and HCN during the ARCTAS-CARB 2008 campaign. The slope of the linear regression is 2.5, with $R^2 = 0.84$.

the measurement of glycolaldehyde more than the measurement of hydroxyacetone.

4 Observations

Aircraft observations indicate a range of glycolaldehyde concentrations in California. Low altitude (<1.5 km pressure altitude) DC-8 flight tracks over northern and central California colored by observed glycolaldehyde concentrations are shown in Fig. 5. Observed concentrations range from several hundred pptv along the coast to concentrations greater than 10 ppbv further inland, closer to biomass-burning and biogenic sources. Ground-based measurements of hydroxyacetone, glycolaldehyde, and acetic acid concentrations during BEARPEX 2009 are shown in Fig. 6.

5 Results and discussion

5.1 ARCTAS-CARB 2008

During the ARCTAS-CARB 2008 campaign, glycolaldehyde concentrations are well correlated with HCN, an atmospheric tracer of biomass-burning emissions (e.g., Li et al., 2003), as shown in Fig. 7 for low altitude measurements (< 1.5 km pressure altitude). Linear regression, using the York et al. (2004) method that takes into account errors in both the abscissa and ordinate values, gives a slope of 2.5 and $R^2 = 0.84$. Significant glycolaldehyde concentrations occur only in air masses with elevated HCN (≥ 250 pptv).

Individual enhancement ratios (Akagi et al., 2011) were calculated for three biomass-burning plumes in which glycolaldehyde, HCN, and CO were measured. A list of biomass-burning plumes encountered by the DC-8 during the ARCTAS campaign can be found in Hornbrook et al. (2011). Possible biomass-burning plumes are identified by time periods of elevated biomass-burning tracer mixing ratios. Plumes are defined by HCN greater than 400 pptv, acetonitrile (CH_3CN) greater than 200 pptv, and CO greater than 175 ppbv. Elevated mixing ratios of NO_x and toluene, anthropogenic tracers, were used to exclude plumes sampled in urban regions. Multiple samplings of a plume were grouped together and are referred to as a single plume. The plumes analyzed in this work were encountered at 18:27–18:30 UTC (Universal Time Coordinated) and 18:38–18:41 UTC on 18 June, 21:08–21:12 UTC and 21:23–21:44 UTC on 22 June, and 14:32–14:35 UTC, 15:34–16:17 UTC, and 16:39–16:57 UTC on 26 June. The correlation of glycolaldehyde with CO, a long-lived plume tracer, was determined by linear regression using the York et al. (2004) method. Calculated enhancement ratios, associated R^2 values, and the estimated plume age of the three plumes are given in Table 1.

A number of studies have reported emission ratios or emission factors for laboratory and field measurements of glycolaldehyde from biomass burning (Akagi et al., 2011, 2012; Yokelson et al., 2013; Johnson et al., 2013). The observed fires span a range of fuel types and modified combustion efficiencies (MCE). Emission ratios range from 14 (pptv glycolaldehyde / ppbv CO) for a tropical forest (Akagi et al., 2011) to 1.87×10^{-2} for chaparral in California (Akagi et al., 2012), with most values between 1 and 10. The mean calculated enhancement ratio of glycolaldehyde for the biomass-burning plumes encountered in California and discussed in this work is 5.7. These ratios were determined for fires with different plume ages and various fuel types. Post-emission chemistry is expected to affect enhancement ratios, and

Table 1. Calculated enhancement ratios and the associated R^2 values (given in parentheses) of HCN and glycolaldehyde (GLYC) relative to long-lived plume tracer CO for three biomass-burning plumes encountered during the 2008 ARCTAS-CARB campaign.

Flight date	$\frac{\Delta GLYC(pptv)}{\Delta CO\ (ppbv)}$	Plume age (days)[a]
18 June	4.6 (0.91)	1
22 June	5.7 (0.56)	0.1
26 June	6.8 (0.93)	1

[a] Hornbrook et al. (2011).

previous work has observed an increase in glycolaldehyde relative to CO with plume age (Akagi et al., 2012). The ARCTAS-CARB observations are consistent with the previously reported observations of glycolaldehyde in biomass-burning plumes.

5.2 BEARPEX 2009

The BEARPEX ground site is located on the western slope of the Sierra Nevada in a ponderosa pine plantation. The site is approximately 5 h downwind of Sacramento, and a band of oak forest is located approximately halfway between Sacramento and the site. The prevailing daytime wind pattern transports anthropogenic volatile organic compounds (VOCs) and NO_x emissions from Sacramento and the Central Valley to the site. Isoprene, emitted from the band of oak forest, and MBO, emitted locally by the ponderosa pine forest, are added to the mixture. Wind direction reverses at night and brings clean air from the mountains to the site. Further details of the BEARPEX site can be found in Goldstein et al. (2000) and Dreyfus et al. (2002).

Hydroxyacetone and glycolaldehyde concentrations are well correlated during the BEARPEX 2009 campaign (Fig. 8). The slope of the linear regression is 1.42 ± 0.01, and the intercept is -1.9 ± 5 pptv, with $R^2 = 0.91$. The high correlation is consistent with the hypothesis that hydroxyacetone and glycolaldehyde have similar sources (isoprene second-generation photooxidation) and sinks (reaction with OH and photolysis). The average ambient temperature was ~5 K higher for days after the day-of-year (DOY) 195 compared to those prior (Fig. 6). This is a likely explanation for the increase in observed hydroxyacetone, glycolaldehyde, and acetic acid concentrations after DOY 195 as emissions of isoprene and MBO are light and temperature dependent (Baker et al., 1999; Lamanna et al., 1999; Schade et al., 2000; Schade and Goldstein, 2001; Gray et al., 2005). The mean hydroxyacetone concentration measured during BEARPEX 2009 was 774 pptv, and the mean glycolaldehyde concentration was 986 pptv. Spaulding et al. (2003) measured similar hydroxyacetone and glycolaldehyde concentrations (420 and 690 pptv, respectively) during an 8-day sampling period at the same site in August and September of 2000.

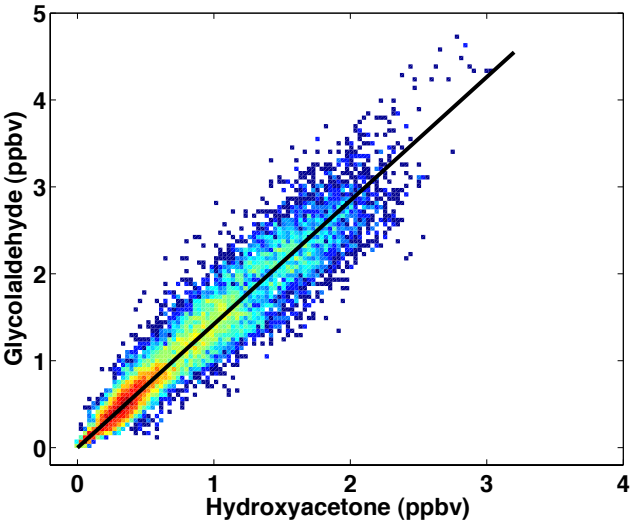

Fig. 8. Correlation between glycolaldehyde and hydroxyacetone during the BEARPEX 2009 campaign. Point color represents data density, with hotter colors being higher density. The slope of the linear regression is 1.42, and the intercept is −1.9 pptv. R^2 = 0.91. The correlation is consistent with the hypothesis that hydroxyacetone and glycolaldehyde have similar sources and sinks.

A simple box model was employed to provide the context for the BEARPEX measurements of glycolaldehyde and hydroxyacetone. VOCs represented in the model are isoprene and MBO; the concentrations of these VOCs simulate an isoprene source between Sacramento and the measurement site (the suburban oak tree belt) and a local source of MBO from the ponderosa pine plantation. The model was developed such that emissions from Sacramento (located at time 0) and the suburban oak tree belt (located at time ≈ 150 min) are processed en route to the BEARPEX site (located at time ≈ 300 min). The magnitude of the emissions is constructed such that the concentrations of isoprene and MBO are consistent with measurements conducted at the site. The time chosen as representative of the measurement site, 300 min, consistent with a 5 h transport time from Sacramento to the site. Modeled concentrations of isoprene and MBO are shown in Fig. 9a. At 300 min, isoprene and MBO concentrations are both 2 ppbv.

Reaction rate constants are taken from IUPAC (International Union of Pure and Applied Chemistry) (Atkinson et al., 2004, 2006) and JPL (Jet Propulsion Laboratory) (Sander et al., 2006) compilations. The rate constants for the reactions of isoprene-derived RO_2 and HO_2 suggested by Jenkin et al. (1997) have been used. Photolysis rates were calculated using the Tropospheric Ultraviolet and Visible (TUV) radiation model (http://cprm.acd.ucar.edu/Models/TUV/). The isoprene oxidation mechanisms of Paulot et al. (2009a, b) have been followed with modifications and additions to mechanisms based on recent laboratory chamber experiments. The yield of hydroxyacetone from methacrolein

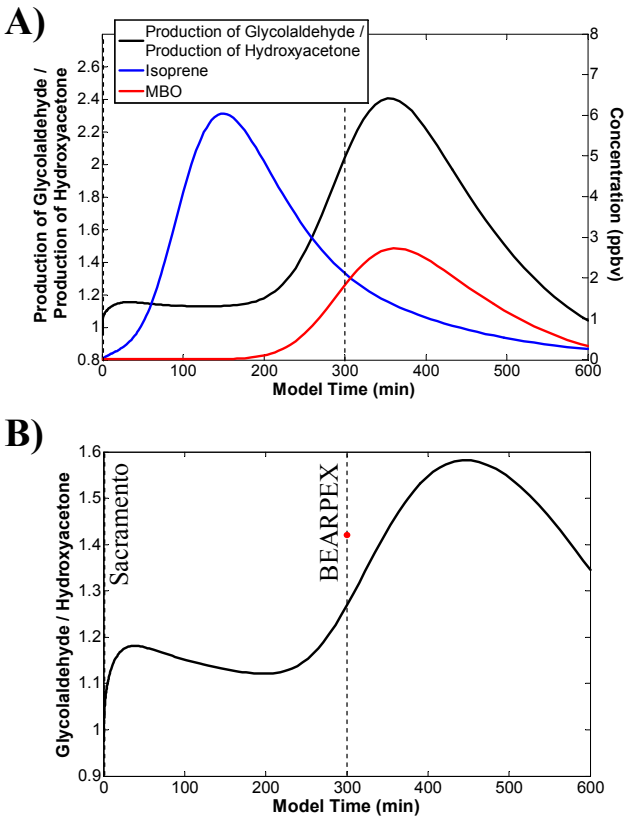

Fig. 9. Ratio of the production of glycolaldehyde to the production of hydroxyacetone and concentration of isoprene and MBO **(A)** as predicted by a simple box model of the BEARPEX 2009 campaign. Ratio of glycolaldehyde concentration to hydroxyacetone concentration **(B)**. As the BEARPEX site is approximately 5 h downwind of Sacramento, CA, model oxidation time of 300 min is expected to correspond to site conditions. The observed ratio of glycolaldehyde to hydroxyacetone is marked at 300 min (red dot).

oxidation in the presence of NO_x has been increased to 0.43, consistent with the findings of Orlando et al. (1999) and Galloway et al. (2011). The mechanism describing MBO oxidation in the presence of NO_x from Chan et al. (2009) has been followed. A 0.15 yield of glycolaldehyde from MBO oxidation under low-NO_x conditions has been used as suggested by recent laboratory chamber experiments performed at Caltech. A unimolecular isomerization pathway from the hydroxyperoxy radical of MACR that yields hydroxyacetone has been added and is the dominant formation pathway for hydroxyacetone in the model (Crounse et al., 2012). The model includes a smaller yield of hydroperoxide (0.3) from MVK $RO_2 + HO_2$ chemistry than recommended by the Master Chemical Mechanism, MCM v3.2 (Jenkin et al., 1997; Saunders et al., 2003), and a large yield (0.6) of glycolaldehyde. The model does not include deposition.

Absolute concentrations of glycolaldehyde and hydroxyacetone calculated by the model are 1.1 and 0.9 ppbv, respectively, at 300 min and are similar to the mean observations from the campaign. The ratio of the glycolaldehyde concentration to hydroxyacetone concentration predicted by the model is shown in Fig. 9b. The predicted ratio resulting from only isoprene oxidation ranges from 1.1 to 1.2. The initial ratio is determined by the prompt formation of glycolaldehyde and hydroxyacetone via radical rearrangement as proposed by theoretical work (Dibble, 2004a, b; Peeters and Nguyen, 2012) and recent laboratory chamber experiments (Paulot et al., 2009a; Galloway et al., 2011) and suggested by field observations (Karl et al., 2009). The ratio increases when glycolaldehyde from MVK oxidation and hydroxyacetone from MACR oxidation are the dominant formation pathways. Since glycolaldehyde is formed from MBO oxidation and hydroxyacetone is not, the glycolaldehyde / hydroxyacetone ratio increases from 1.2 to 1.6 as more MBO is oxidized to form glycolaldehyde (250–600 min). The ratio of the production rate of glycolaldehyde to that of hydroxyacetone is shown in Fig. 9a and is mostly affected by increased glycolaldehyde production from MBO oxidation. Late in the model, oxidation of dihydroxyepoxides (IEPOX) of isoprene contributes to both hydroxyacetone and glycolaldehyde concentrations (Bates et al., 2014), highlighting the potential importance of the late-generation isoprene oxidation chemistry at the site. The observed ratio of glycolaldehyde to hydroxyacetone at the BEARPEX site is 1.4 (Fig. 8), indicating predictions based only on isoprene and MBO chemistry are consistent with observations.

6 Conclusions

Chemical ionization mass spectrometry provides robust detection and quantification of hydroxyacetone and glycolaldehyde. The Caltech single quadrupole and tandem mass spectrometers are equally capable of the measurement of hydroxyacetone. Tandem mass spectrometry provides direct separation of the daughter ions of glycolaldehyde and acetic acid, enabling the differentiation of these mass analogues. This online method enables fast, in situ measurements with no sample processing. Ambient measurements of glycolaldehyde were conducted during the ARCTAS-CARB 2008 campaign using the Caltech single quadrupole CIMS instrument. Enhancement ratios of glycolaldehyde were calculated for three biomass-burning plumes encountered in California during June 2008. Ambient measurements of hydroxyacetone and glycolaldehyde concentrations from the oxidation of biogenic emissions were conducted during the BEARPEX 2009 campaign using the Caltech tandem CIMS instrument. The observed ratio of glycolaldehyde to hydroxyacetone mixing ratios is consistent with predictions from a simple box model in which isoprene and MBO are the only VOCs represented.

Acknowledgements. G. S. Diskin and G. W. Sachse provided ARCTAS-CARB water measurements and CO measurements. BEARPEX 2009 water measurements were provided by A. H. Goldstein. Isoprene and MBO measurements were provided by G. W. Schade. The authors wish to thank the ARCTAS-CARB science team, the DC-8 crew, and the ARCTAS-CARB support team. The authors also wish to thank the BEARPEX science team and the UC Blodgett Forest Research staff. The hydroxyacetone, glycolaldehyde, and acetic acid measurements and their interpretation were made possible with the financial support of NASA (NAG: NNX-08AD29G) and the NSF (ATM-0934408).

Edited by: V. F. McNeill

References

Akagi, S. K., Yokelson, R. J., Wiedinmyer, C., Alvarado, M. J., Reid, J. S., Karl, T., Crounse, J. D., and Wennberg, P. O.: Emission factors for open and domestic biomass burning for use in atmospheric models, Atmos. Chem. Phys., 11, 4039–4072, doi:10.5194/acp-11-4039-2011, 2011.

Akagi, S. K., Craven, J. S., Taylor, J. W., McMeeking, G. R., Yokelson, R. J., Burling, I. R., Urbanski, S. P., Wold, C. E., Seinfeld, J. H., Coe, H., Alvarado, M. J., and Weise, D. R.: Evolution of trace gases and particles emitted by a chaparral fire in California, Atmos. Chem. Phys., 12, 1397–1421, doi:10.5194/acp-12-1397-2012, 2012.

Amelynck, C., Van Bavel, A. M., Schoon, N., and Arijs, E.: Gas phase reactions of CF_3O^- and $CF_3O^- \cdot H_2O$ and their relevance to the detection of stratospheric HCl, Int. J. Mass Spectrom., 202, 207–216, 2000a.

Amelynck, C., Schoon, N., and Arijs, E.: Gas phase reactions of CF_3O^- and $CF_3O^- \cdot H_2O$ with nitric, formic, and acetic acid, Int. J. Mass Spectrom., 203, 165–175, 2000b.

Atkinson, R., and Arey, J.: Gas-phase tropospheric chemistry of biogenic volatile organic compounds: A review, Atmos. Environ., 37, S197–S219, doi:10.1016/S1352-2310(03)00391-1, 2003.

Atkinson, R., Baulch, D. L., Cox, R. A., Crowley, J. N., Hampson, R. F., Hynes, R. G., Jenkin, M. E., Rossi, M. J., and Troe, J.: Evaluated kinetic and photochemical data for atmospheric chemistry: Volume I – gas phase reactions of O_x, HO_x, NO_x and SO_x species, Atmos. Chem. Phys., 4, 1461–1738, doi:10.5194/acp-4-1461-2004, 2004.

Atkinson, R., Baulch, D. L., Cox, R. A., Crowley, J. N., Hampson, R. F., Hynes, R. G., Jenkin, M. E., Rossi, M. J., and Troe, J.: Evaluated kinetic and photochemical data for atmospheric chemistry: Volume II – gas phase reactions of organic species, Atmos. Chem. Phys., 6, 3625–4055, doi:10.5194/acp-6-3625-2006, 2006.

Baker, B., Guenther, A., Greenberg, J., Goldstein, A., and Fall, R.: Canopy fluxes of 2-methyl-3-buten-2-ol over a ponderosa pine forest by relaxed eddy accumulation: Field data and model comparison, J. Geophys. Res.-Atmos., 104, 26107–26114, 1999.

Bates, H. B., Crounse, J. D., St. Clair, J. M., Bennett, N. B., Nguyen, T. B., Seinfeld, J. H., Stoltz, B. M., and Wennberg, P. O.: Gas phase production and loss of isoprene epoxydiols, J. Phys. Chem. A, 118, 1237—1246, doi:10.1021/jp4107958, 2014.

Butkovskaya, N. I., Pouvesle, N., Kukui, A., and Le Bra, G.: Mechanism of the OH-initiated oxidation of glycolaldehyde over the temperature range 233–296 K, J. Phys. Chem. A, 110, 13492–13499, doi:10.1021/JP064993K, 2006a.

Butkovskaya, N. I., Pouvesle, N., Kukui, A., Mu, Y. J., and Le Bras, G.: Mechanism of the OH-initiated oxidation of hydroxyacetone over the temperature range 236–298 K, J. Phys. Chem. A, 110, 6833–6843, doi:10.1021/JP056345R, 2006b.

Chameides, W. L., Lindsay, R. W., Richardson, J., and Kiang, C. S.: The role of biogenic hydrocarbons in urban photochemical smog: Atlanta as a case study, Science, 241, 1473–1475, 1988.

Chan, A. W. H., Galloway, M. M., Kwan, A. J., Chhabra, P. S., Keutsch, F. N., Wennberg, P. O., Flagan, R. C., and Seinfeld, J. H.: Photooxidation of 2-Methyl-3-Buten-2-ol (MBO) as a potential source of secondary organic aerosol, Environ. Sci. Technol., 43, 4647–4652, doi:10.1021/ES802560W, 2009.

Crounse, J. D., McKinney, K. A., Kwan, A. J., and Wennberg, P. O.: Measurement of gas-phase hydroperoxides by chemical ionization mass spectrometry, Anal. Chem., 78, 6726–6732, 2006.

Crounse, J. D., DeCarlo, P. F., Blake, D. R., Emmons, L. K., Campos, T. L., Apel, E. C., Clarke, A. D., Weinheimer, A. J., McCabe, D. C., Yokelson, R. J., Jimenez, J. L., and Wennberg, P. O.: Biomass burning and urban air pollution over the Central Mexican Plateau, Atmos. Chem. Phys., 9, 4929–4944, doi:10.5194/acp-9-4929-2009, 2009.

Crounse, J. D., Knap, H. C., Ornso, K. B, Jorgensen, S., Paulot, F., Kjaergaard, H. G., and Wennberg, P. O.: Atmospheric fate of methacrolein. 1. peroxy radical isomerization following addition of OH and O_2, J. Phys. Chem. A, 9, 5756–5762, doi:10.1021/jp211560u, 2012.

Dibble, T. S.: Intramolecular hydrogen bonding and double H-atom transfer in peroxy and alkoxy radicals from isoprene, J. Phys. Chem. A, 108, 2199–2207, doi:10.1021/JP0306702, 2004a.

Dibble, T. S.: Prompt chemistry of alkenoxy radical products of the double H-atom transfer of alkoxy radicals from isoprene, J. Phys. Chem. A, 108, 2208–2215, doi:10.1021/JP0312161, 2004b.

Dreyfus, G. B., Schade, G. W., and Goldstein, A. H.: Observational constraints on the contribution of isoprene oxidation to ozone production on the western slope of the Sierra Nevada, California, J. Geophys. Res.-Atmos., 107, 4365, doi:10.1029/2001JD001490, 2002.

Galloway, M. M., Huisman, A. J., Yee, L. D., Chan, A. W. H., Loza, C. L., Seinfeld, J. H., and Keutsch, F. N.: Yields of oxidized volatile organic compounds during the OH radical initiated oxidation of isoprene, methyl vinyl ketone, and methacrolein under high NO_x conditions, Atmos. Chem. Phys., 11, 10779–10790, doi:10.5194/acp-11-10779-2011, 2011.

Goldan, P. D., Kuster, W. C., Fehsenfeld, F. C., and Montzka, S. A.: The observation of a C_5 alcohol emission in a North American pine forest, Geophysical Research Letters, 20, 1039–1042, 1993.

Goldstein, A. H., Hultman, N. E., Fracheboud, J. M., Bauer, M. R., Panek, J. A., Xu, M., Qi, Y., Guenther, A. B., and Baugh, W.: Effects of climate variability on the carbon dioxide, water, and sensible heat fluxes above a ponderosa pine plantation in the Sierra Nevada (CA), Agr. Forest Meteorol., 101, 113–129, 2000.

Gray, D. W., Goldstein, A. H., and Lerdau, M. T.: The influence of light environment on photosynthesis and basal methylbutenol emission from *Pinus ponderosa*, Plant Cell Environ., 28, 1463–1474, 2005.

Griffith, D. W. T.: Synthetic calibration and quantitative analysis of gas-phase FT-IR spectra, Appl. Spectrosc., 50, 59–70, 1996.

Grosjean, D., Williams, E. L., and Grosjean, E.: Atmospheric chemistry of isoprene and of its carbonyl products, Environ. Sci. Technol., 27, 830–840, 1993.

Guenther, A., Hewitt, C. N., Erickson, D., Fall, R., Geron, C., Graedel, T., Harley, P., Klinger, L., Lerdau, M., McKay, W. A., Pierce, T., Scholes, B., Steinbrecher, R., Tallamraju, R., Taylor, J., and Zimmerman, P.: A global-model of natural volatile organic-compound emissions, J. Geophys. Res.-Atmos., 100, 8873–8892, 1995.

Harley, P., Fridd-Stroud, V., Greenberg, J., Guenther, A., and Vasconcellos, P.: Emission of 2-methyl-3-buten-2-ol by pines: A potentially large natural source of reactive carbon to the atmosphere, J. Geophys. Res.-Atmos., 103, 25479–25486, 1998.

Hornbrook, R. S., Blake, D. R., Diskin, G. S., Fuelberg, H. E., Meinardi, S., Mikoviny, T., Sachse, G. W., Vay, S. A., Weinheimer, A. J., Wiedinmyer, C., Wisthaler, A., Hills, A., Riemer, D. D., and Apel, E. C.: Observations of volatile organic compounds during ARCTAS – Part 1: Biomass burning emissions and plume enhancements, Atmos. Chem. Phys., 11, 11103–11130, doi:10.5194/acp-11-11103-2011, 2011.

Huey, L. G., Villalta, P. W., Dunlea, E. J., Hanson, D. R., and Howard, C. J.: Reactions of CF_3O^- with atmospheric trace gases, J. Phys. Chem., 100, 190–194, 1996.

Jenkin, M. E., Saunders, S. M., and Pilling, M. J.: The tropospheric degradation of volatile organic compounds: A protocol for mechanism development, Atmos. Environ., 31, 81–104, 1997.

Johnson, T. J., Sams, R. L., Profeta, L. T. M., Akagi, S. K., Burling, I. R., Yokelson, R. J., Williams, S. D.: Quantitative IR spectrum and vibrational assignments for glycolaldehyde vapor: glycolaldehyde measurements in biomass burning plumes, J. Phys. Chem. A, 117, 4096–4107, doi:/10.1021/jp311945p, 2013.

Karl, T., Guenther, A., Turnipseed, A., Tyndall, G., Artaxo, P., and Martin, S.: Rapid formation of isoprene photo-oxidation products observed in Amazonia, Atmos. Chem. Phys., 9, 7753–7767, doi:10.5194/acp-9-7753-2009, 2009.

Kroll, J. H., Ng, N. L., Murphy, S. M., Flagan, R. C., and Seinfeld, J. H.: Secondary organic aerosol formation from isoprene photooxidation, Environ. Sci. Technol., 40, 1869–1877, doi:10.1021/ES0524301, 2006.

Lamanna, M. S., and Goldstein, A. H.: In situ measurements of C_2–C_{10} volatile organic compounds above a Sierra Nevada ponderosa pine plantation, J. Geophys. Res.-Atmos., 104, 21247–21262, 1999.

Lee, Y. N., and Zhou, X. L.: Method for the determination of some soluble atmospheric carbonyl compounds, Environ. Sci. Technol., 27, 749–756, 1993.

Lee, Y. N., Zhou, X. L., and Hallock, K.: Atmospheric carbonyl compounds at a rural Southeastern U.S. site, J. Geophys. Res.-Atmos., 100, 25933–25944, 1995.

Li, Q. B., Jacob, D. J., Yantosca, R. M., Heald, C. L., Singh, H. B., Koike, M., Zhao, Y. J., Sachse, G. W., and Streets, D. G.: A global three-dimensional model analysis of the atmospheric budgets of HCN and CH_3CN: Constraints from aircraft and ground measurements, J. Geophys. Res.-Atmos., 108, 8827, doi:10.1029/2002JD003075, 2003.

Matsunaga, S., Mochida, M., and Kawamura, K.: Growth of organic aerosols by biogenic semi-volatile carbonyls in the forestal atmosphere, Atmos. Environ., 37, 2045–2050, doi:10.1016/S1352-2310(03)00089-X, 2003.

Moortgat, G. K., Grossmann, D., Boddenberg, A., Dallmann, G., Ligon, A. P., Turner, W. V., Gab, S., Slemr, F., Wieprecht, W., Acker, K., Kibler, M., Schlomski, S., and Bachmann, K.: Hydrogen peroxide, organic peroxides and higher carbonyl compounds determined during the BERLIOZ campaign, J. Atmos. Chem., 42, 443–463, 2002.

Niki, H., Maker, P. D., Savage, C. M., and Hurley, M. D.: Fourier transform infrared study of the kinetics and mechanisms for the Cl-atom- and HO-radical-initiated oxidation of glycolaldehyde, J. Phys. Chem., 91, 2174–2178, 1987.

Orlando, J. J., Tyndall, G. S., Fracheboud, J. M., Estupinan, E. G., Haberkorn, S., and Zimmer, A.: The rate and mechanism of the gas-phase oxidation of hydroxyacetone, Atmos. Environ., 33, 1621–1629, 1999.

Paulson, S. E., Flagan, R. C., and Seinfeld, J. H.: Atmospheric photooxidation of isoprene Part 1: The hydroxyl radical and ground-state atomic oxygen reactions, Int. J. Chem. Kin., 24, 79–101, 1992.

Paulot, F., Crounse, J. D., Kjaergaard, H. G., Kroll, J. H., Seinfeld, J. H., and Wennberg, P. O.: Isoprene photooxidation: New insights into the production of acids and organic nitrates, Atmos. Chem. Phys., 9, 1479–1501, doi:10.5194/acp-9-1479-2009, 2009a.

Paulot, F., Crounse, J. D., Kjaergaard, H. G., Kurten, A., St. Clair, J. M., Seinfeld, J. H., and Wennberg, P. O.: Unexpected epoxide formation in the gas-phase photooxidation of isoprene, Science, 325, 730–733, doi:10.1126/science.1172910, 2009b.

Peeters, J. and Nguyen, T. L.: Unusually fast 1,6-H shifts of enolic hydrogens in peroxy radicals: formation of the first-generation C_2 and C_3 carbonyls in the oxidation of isoprene, J. Phys. Chem. A, 116, 6134–6141, doi:10.1021/jp211447q, 2012.

Rothman, L. S., Jacquemart, D., Barbe, A., Benner, D. C., Birk, M., Brown, L. R., Carleer, M. R., Chackerian, C., Chance, K., Coudert, L. H., Dana, V., Devi, V. M., Flaud, J. M., Gamache, R. R., Goldman, A., Hartmann, J. M., Jucks, K. W., Maki, A. G., Mandin, J. Y., Massie, S. T., Orphal, J., Perrin, A., Rinsland, C. P., Smith, M. A. H., Tennyson, J., Tolchenov, R. N., Toth, R. A., Vander Auwera, J., Varanasi, P., and Wagner, G.: The HITRAN 2004 molecular spectroscopic database, J. Quant. Spectrosc. Radiat. Transf., 96, 139–204, 2005.

Sander, S. P., Friedl, R. R., Golden, D. M., Kurylo, M. J., Moortgat, G. K., Keller-Rudek, H., Wine, P. H., Ravishankara, A. R., Kolb, C. E., Molina, M. J., Finlayson-Pitts, B. J., Huie, R. E., and Orkin, V. L.: Chemical Kinetics and Photochemical Data for Use in Atmospheric Studies, Evaluation Number 15 JPL Publication 06-2, NASA Jet Propulsion Laboratory, California Institute of Technology, Pasadena, CA, 2006.

Saunders, S. M., Jenkin, M. E., Derwent, R. G., and Pilling, M. J.: Protocol for the development of the Master Chemical Mechanism, MCM v3 (Part A): Tropospheric degradation of non-aromatic volatile organic compounds, Atmos. Chem. Phys., 3, 161–180, doi:10.5194/acp-3-161-2003, 2003.

Schade, G. W., Goldstein, A. H., Gray, D. W., and Lerdau, M. T.: Canopy and leaf level 2-methyl-3-buten-2-ol fluxes from a ponderosa pine plantation, Atmos. Environ., 34, 3535–3544, 2000.

Schade, G. W., and Goldstein, A. H.: Fluxes of oxygenated volatile organic compounds from a ponderosa pine plantation, J. Geophys. Res.-Atmos., 106, 3111–3123, 2001.

Spaulding, R. S., Schade, G. W., Goldstein, A. H., and Charles, M. J.: Characterization of secondary atmospheric photooxidation products: Evidence for biogenic and anthropogenic sources, J. Geophys. Res.-Atmos., 108, 4247, doi:10.1029/2002JD002478, 2003.

Spencer, K. M., McCabe, D. C., Crounse, J. D., Olson, J. R., Crawford, J. H., Weinheimer, A. J., Knapp, D. J., Montzka, D. D., Cantrell, C. A., Hornbrook, R. S., Mauldin, R. L., and Wennberg, P. O.: Inferring ozone production in an urban atmosphere using measurements of peroxynitric acid, Atmos. Chem. Phys., 9, 3697–3707, doi:10.5194/acp-9-3697-2009, 2009.

St. Clair, J. M., McCabe, D. C., Crounse, J. D., Steiner, U., and Wennberg, P. O.: Chemical ionization tandem mass spectrometer for the in situ measurement of methyl hydrogen peroxide, Rev. Sci. Inst., 81, 094102, doi:10.1063/1.3480552, 2010.

Tuazon, E. C., and Atkinson, R.: A product study of the gas-phase reaction of methyl vinyl ketone with the OH radical in the presence of NO_x, Int. J. Chem. Kin., 21, 1141–1152, 1989.

Tuazon, E. C., and Atkinson, R.: A product study of the gas-phase reaction of isoprene with the OH radical in the presence of NO_x, Int. J. Chem. Kin., 22, 1221–1236, 1990a.

Tuazon, E. C., and Atkinson, R.: A product study of the gas-phase reaction of methacrolein with the OH radical in the presence of NO_x, Int. J. Chem. Kin., 22, 591–602, 1990b.

Washenfelder, R. A., Roehl, C. M., McKinney, K. A., Julian, R. R., and Wennberg, P. O.: A compact, lightweight gas standards generator for permeation tubes, Rev. Sci. Inst., 74, 3151–3154, doi:10.1063/1.1570949, 2003.

Yokelson, R. J., Burling, I. R., Gilman, J. B., Warneke, C., Stockwell, C. E., de Gouw, J. , Akagi, S. K., Urbanski, S. P., Veres, P., Roberts, J. M., Kuster, W. C., Reardon, J., Griffith, D. W. T., Johnson, T. J., Hosseini, S., Miller, J. W., Cocker III, D. R., Jung, H., and Weise, D. R.: Coupling field and laboratory measurements to estimate the emission factors of identified and unidentified trace gases for prescribed fires, Atmos. Chem. Phys., 13, 89–116, doi:10.5194/acp-13-89-2013, 2013.

York, D., Evensen, N. M., Martinez, M. L., and Delgado, J. D.: Unified equations for the slope, intercept, and standard errors of the best straight line, Am. J. Phys., 72, 367–375, doi:10.1119/1.1632486, 2004.

Zhou, X. L., Huang, G., Civerolo, K., and Schwab, J.: Measurement of atmospheric hydroxyacetone, glycolaldehyde, and formaldehyde, Environ. Sci. Technol., 43, 2753–2759, doi:10.1021/ES803025G, 2009.